Global Energy Interconnection
Development and Cooperation Organization

Volume 3 Number 4 August 2020 (365-374)
DOI: 10.14171/j.2096-5117.gei.2020.04.007

Global Energy Interconnection

Contents lists available at ScienceDirect
https: //www.sciencedirect.com/journal/global-energy-interconnection

ELSEVIER Production And Hosting By Elsevier On Behalf Of KeAi

Full-length article

Coordinated voltage control of renewable energy power plants in weak sending-end power grid

Yongning Chi[1], Weihao Li[2], Qiuwei Wu[2,3], Chao Liu[1]

1. Department of Renewable Energy, China Electric Power Research Institute, Beijing 100031, P.R. China
2. School of Electrical Engineering, Shandong University, Jinan 250000, P.R. China
3. Center for Electric Power and Energy, Department of Electrical Engineering, Technical University of Denmark, Kgs. Lyngby, Denmark

Scan for more details

Abstract: The utilization of renewable energy in sending-end power grids is increasing rapidly, which brings difficulties to voltage control. This paper proposes a coordinated voltage control strategy based on model predictive control (MPC) for the renewable energy power plants of wind and solar power connected to a weak sending-end power grid (WSPG). Wind turbine generators (WTGs), photovoltaic arrays (PVAs), and a static synchronous compensator are coordinated to maintain voltage within a feasible range during operation. This results in the full use of the reactive power capability of WTGs and PVAs. In addition, the impact of the active power outputs of WTGs and PVAs on voltage control are considered because of the high R/X ratio of a collector system. An analytical method is used for calculating sensitivity coefficients to improve computation efficiency. A renewable energy power plant with 80 WTGs and 20 PVAs connected to a WSPG is used to verify the proposed voltage control strategy. Case studies show that the coordinated voltage control strategy can achieve good voltage control performance, which improves the voltage quality of the entire power plant.

Keywords: Coordinated voltage control, Model predictive control (MPC), Renewable energy, Weak sending-end power grid, Wind turbine generators (WTGs), Photovoltaic arrays (PVAs), STATCOM.

1 Introduction

China has gradually increased the development and investment in the field of renewable energy to address the concerns of energy shortage and environmental pollution. Various renewable energy generation technologies have been developed rapidly in the past few years, particularly wind power and photovoltaic (PV) power. Currently, there are numerous large-scale wind and PV power plants, which are mainly distributed in the “Three North” region of China. Weak sending-end power grids (WSPGs) are typically used for the large-scale development and centralized transmission of renewable energy in the Three North region [1].

A WSPG generally consists of only a few conventional power plants in addition to renewable energy power plants. In a WSPG, the network structure is weak, the

Received: 8 May 2020/ Accepted: 2 July 2020/ Published: 25 August 2020

Yongning Chi
chiyn@epri.sgcc.com.cn

Weihao Li
846102485@qq.com

Qiuwei Wu
quiwudtu@163.com

Chao Liu
liuchao@epri.sgcc.com.cn

2096-5117/© 2020 Global Energy Interconnection Development and Cooperation Organization. Production and hosting by Elsevier B.V. on behalf of KeAi Communications Co., Ltd. This is an open access article under the CC BY-NC-ND license (http: //creativecommons.org/licenses/by-nc-nd/4.0/).

short-circuit capacity is insufficient [2], and the active and reactive power support capacity is low. The spatial and temporal distribution of wind power and solar power has strong volatility and intermittency [3], [4]. The voltage of a WSPG fluctuates frequently owing to the active power output fluctuations of the wind farms and PV power stations connected to the WSPG. This leads to severe challenges in ensuring the stability of power grid voltage. Thus, stringent requirements have been specified for renewable energy power plants, including voltage control performance and the reactive power regulation capability [5].

Owing to the weak reactive power support capacity of WSPGs, it is necessary to fully utilize the reactive power capacity of wind farms and PV power stations to maintain the balance of reactive power. Therefore, it is extremely important to study the reactive power and voltage control strategy of large-scale renewable energy power stations connected to a WSPG. Various devices have been installed in renewable energy power stations to achieve better voltage control performance, e.g., static synchronous compensators (STATCOMs) and static Var compensators [6]. Moreover, with the development of power electronics technologies, renewable energy generation units, including wind turbine generators (WTGs) and PV arrays (PVAs), can be used for voltage control [7]. However, the coordination of reactive power compensation devices with different time constants has become a difficult problem in the voltage control of renewable energy power stations.

Voltage control methods have been proposed for renewable energy power stations. In [8–12], the reactive power reference of a renewable energy power station is obtained according to the voltage deviation at the point of connection (POC) and allocated to generation units based on a proportional distribution. Control strategies based on mathematical programming algorithms are proposed in [13–19]. These strategies describe a voltage control problem as a mathematical optimization problem with constraints, which can be solved using various optimization algorithms. In [13] and [14], a voltage control method based on a dynamic programming algorithm is developed for wind farms. The method can effectively suppress the voltage oscillation of wind farms after large disturbances. In [15], a central controller algorithm that is based on a dynamic programming is presented to realize voltage control for wind farms with the minimum number of capacitor steps operations. In [16–19], voltage control methods based on optimal power flow are studied. These control methods consider not only voltage control performance but also the reduction in active power loss.

The voltage control methods described above are open-loop control methods with a single time section, which does not consider the dynamic regulation process of reactive power compensation devices with different time constants. Unlike the above control methods, model predictive control (MPC) is a rolling optimization control method, which can better deal with the influence of system uncertainty and shows robust voltage control performance. In [20], a voltage control method based on MPC is proposed to coordinate the reactive power of WTGs and static Var generators (SVGs). The control target is to minimize the voltage deviation at the POC and maximize the dynamic reactive power reserve of an SVG. In [21], a hierarchical and coordinated voltage control strategy for wind farms is proposed. In this strategy, the prediction information of different time scales in each layer can be fully utilized, and the control between each layer can be effectively coordinated.

Based on the above analysis, MPC can be used to coordinate a renewable energy generation unit and a reactive power compensation device to control voltage because of the following advantages:

(1) MPC does not require a precise predictive model; this can reduce the difficulty of modeling;

(2) It shows good dynamic performance because it uses a rolling optimization strategy;

(3) It can coordinate various Var devices and renewable energy generation units with different time constants [22].

The main contribution of this paper is proposing an MPC-based coordinated voltage control strategy for renewable energy power plants in WSPG, which optimally coordinates WTGs, PVAs, and a STATCOM to balance reactive power and control voltage. The reactive power capability of doubly fed induction generators (DFIGs) and PV inverters is examined. Compared to existing research, the proposed control strategy can realize power control of different generation units and reactive compensation devices with different time constants by using MPC. And an analytical method is used for calculating sensitivity coefficients which improves computation efficiency. Besides, the impacts of the active power output of WTGs and PVAs on voltage variation are considered for achieving better voltage control performance.

The rest of this paper is organized as follows: The topology of the renewable energy power plant and the structure of the voltage control strategy are provided in Section 2. The calculation of sensitivity coefficients is described in Section 3. The predictive model of the entire system is presented in Section 4. Section 5 presents the formulation of the MPC problem. Case studies are discussed in Section 6. Finally, the conclusions are presented in Section 7.

2 Renewable energy power plant and voltage control strategy

2.1 Layout of the renewable energy power plant

Fig. 1 illustrates the configuration of a 360 MW renewable energy power plant consisting of a 320 MW wind farm and a 40 MW PV power station. The wind farm is comprised of four parts connected to four AC collector substations. The four substations are located at distances of 5 km, 10 km, 15 km, and 20 km from the POC. There are twenty 4 MW double-fed WTGs in each part. The WTGs are placed at a distance of 0.5 km with each other. The PV power station comprises twenty 2 MW PVAs. It is connected to an AC collector substation and placed at a distance of 25 km from the POC. The PVAs are placed at a distance of 0.3 km with each other. A ±180 MVar STATCOM located at the POC is selected as the reactive compensation device.

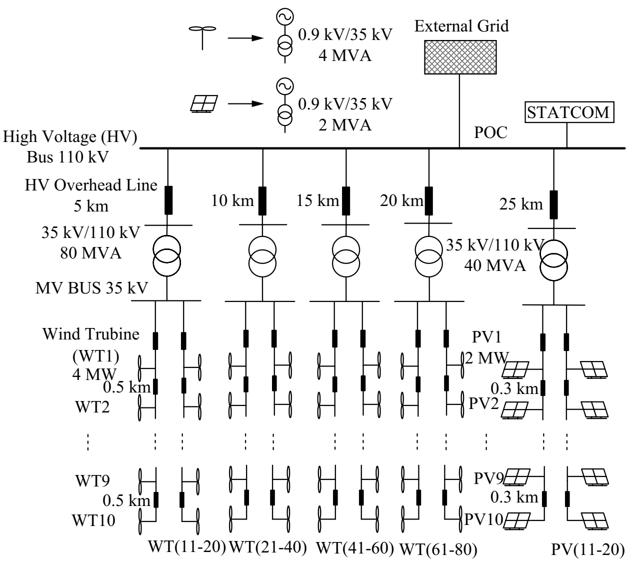

Fig. 1 Configuration of the renewable energy power plant

2.2 Control process

Fig. 2 shows the structure of the voltage control strategy. The measurements of node voltage, the active and reactive power output of each WTG and PVA, and the reactive power output of the STATCOM are transmitted to an MPC controller. Sensitivity coefficients are calculated based on an admittance matrix and the node voltage measurement. The weight coefficients of subobjective functions are calculated using the analytic hierarchy process (AHP) to achieve better voltage control performance. The MPC problem is formulated based on the active power references determined by a system operator, the calculated sensitivity coefficients and weight, and the abovementioned measurements. The details of the MPC problem formulation are presented in Section 5. After solving the MPC problem, the control commands for the WTGs (P_W^{ref}, Q_W^{ref}), PVAs (P_{PV}^{ref}, Q_{PV}^{ref}), and STATCOM (Q_{ST}^{ref}) are delivered to their local controllers.

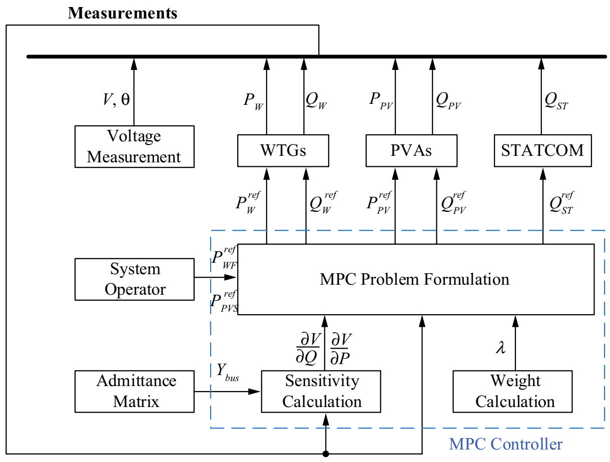

Fig. 2 Structure of the control strategy

3 Sensitivity coefficient calculation

In this section, the calculation of voltage sensitivity coefficients with respect to a power injection is presented.

The conventional method of calculating voltage sensitivity coefficients uses a Jacobian matrix, which must be rebuilt and inversed as operating conditions change. This inevitably decreases computation speed. To improve computation efficiency, an analytical calculation method that was initially applied to a radial distribution grid [23] is adopted in this study.

A power grid with N buses is considered. Γ represents the set of the buses, $\Gamma=\{1,2,\ldots,N\}$. Node voltage is defined as $\overline{V_i} = V_i e^{j\theta_i}$, and the apparent power injection is defined as $\overline{S_i} = P_i + jQ_i$, for $i \in \Gamma$. The apparent power injection can be obtained as follows:

$$\underline{S_i} = \underline{V_i} \sum_{j\in\Gamma} \overline{Y_{bus,ij}}\,\overline{V_j} = P_i - jQ_i \tag{1}$$

where $\underline{S_i}$ and $\underline{V_i}$ represent the conjugates of $\overline{S_i}$ and $\overline{V_i}$, respectively. $\overline{Y_{bus,ij}}$ is an element of admittance matrix $\overline{Y_{bus}}$.

Then, the partial derivatives of $\underline{S_i}$ with respect to active power P_l and reactive power Q_l at bus $l \in \Gamma$ must be obtained in advance for the derivation of the voltage sensitivity coefficients with respect to the active and reactive power injections,

$$\begin{aligned}\frac{\partial \underline{S_i}}{\partial P_l} &= \frac{\partial (P_i - jQ_i)}{\partial P_l} = \begin{cases}1, & i = l\\ 0, & i \neq l\end{cases}\\ &= \frac{\partial \underline{V_i}}{\partial P_l}\sum_{j\in\Gamma}\overline{Y_{bus,ij}}\,\overline{V_j} + \underline{V_i}\sum_{j\in\Gamma}\overline{Y_{bus,ij}}\frac{\partial \overline{V_j}}{\partial P_l}\end{aligned} \tag{2}$$

$$\frac{\partial S_i}{\partial Q_l}=\frac{\partial(P_i-jQ_i)}{\partial Q_l}=\begin{cases}-j, & i=l\\ 0, & i\neq l\end{cases}$$
$$=\frac{\partial \underline{V_i}}{\partial Q_l}\sum_{j\in\Gamma}\overline{Y_{bus,ij}}\,\overline{V_j}+\underline{V_i}\sum_{j\in\Gamma}\overline{Y_{bus,ij}}\frac{\partial\overline{V_j}}{\partial Q_l} \tag{3}$$

Equation (2) is a linear combination of $\partial\overline{V_i}/\partial P_l$ and $\partial\underline{V_i}/\partial P_l$, and (3) is a linear combination of $\partial\overline{V_i}/\partial Q_l$ and $\partial\underline{V_i}/\partial Q_l$. According to the theorem in [23], (2) and (3) can be solved using a unique method.

After obtaining the value of $\partial\overline{V_i}/\partial P_l$, $\partial\underline{V_i}/\partial P_l$, $\partial\overline{V_i}/\partial Q_l$, and $\partial\underline{V_i}/\partial Q_l$, the voltage sensitivity coefficients can be calculated as

$$\frac{\partial V_i}{\partial P_l}=\frac{1}{V_i}\mathrm{Re}(\underline{V_i}\frac{\partial\overline{V_i}}{\partial P_l}) \tag{4}$$

$$\frac{\partial V_i}{\partial Q_l}=\frac{1}{V_i}\mathrm{Re}(\underline{V_i}\frac{\partial\overline{V_i}}{\partial Q_l}) \tag{5}$$

At every control step, the sensitivity coefficients are updated with new measured voltages. Additionally, the sensitivity coefficients remain unchanged at every predictive step.

4 Establishment of predictive model

In this section, the predictive models of the WTGs, PVAs, and STATCOM are established for the formulation of the MPC problem.

4.1 Predictive model of WTG

(1) State space of WTG

The control of the active and reactive power of a double-fed WTG can be decoupled through vector control. To facilitate the transformation of the formulated MPC problem into a standard quadratic programming (QP) problem, state vectors, output vectors, and control vectors are expressed as the deviations from the corresponding current measurements. The active and reactive power references of the WTG are Q_{WT}^{ref} and Q_{WT}^{ref}, respectively. The current measurements of active and reactive powers are $P_{WT}(t_0)$ and $Q_{WT}(t_0)$, respectively, where t_0 represents the current time. Then, the control vectors can be expressed as $\Delta P_{WT}^{ref}=P_{WT}^{ref}-P_{WT}(t_0)$ and $\Delta Q_{WT}^{ref}=Q_{WT}^{ref}-Q_{WT}(t_0)$. In steady state, the power control behavior of the WTG can be described as a first-order lag function owing to the time delay of the communication system and control system of the WTG [24],

$$\Delta P_{WT}=\frac{1}{1+s\tau_{WT}^{P}}\Delta P_{WT}^{ref} \tag{6}$$

$$\Delta Q_{WT}=\frac{1}{1+s\tau_{WT}^{Q}}\Delta Q_{WT}^{ref} \tag{7}$$

where τ_{WT}^{P} and τ_{WT}^{Q} are time constants, which are in a range of 1–10 s [25].

Based on the above analysis, the state space of the WTG can be derived as

$$\Delta\dot{P}_{WT}=A_{WT}^{P}\Delta P_{WT}+B_{WT}^{P}\Delta P_{WT}^{ref} \tag{8}$$

$$\Delta\dot{Q}_{WT}=A_{WT}^{Q}\Delta Q_{WT}+B_{WT}^{Q}\Delta Q_{WT}^{ref} \tag{9}$$

where $A_{WT}^{P}=-1/\tau_{WT}^{P}$, $B_{WT}^{P}=1/\tau_{WT}^{P}$, $A_{WT}^{Q}=-1/\tau_{WT}^{Q}$, and $B_{WT}^{Q}=1/\tau_{WT}^{Q}$.

(2) Reactive power capability of DFIG

As the reactive power output of a double-fed WTG is optimized for voltage control, the reactive power capacity of a DFIG must be analyzed.

The stator power output of a DFIG can be obtained as

$$P_S=3\frac{X_M}{X_S}U_S I_R\sin\delta \tag{10}$$

$$Q_S=3\frac{X_M}{X_S}U_S I_R\cos\delta-3\frac{U_S^2}{X_S} \tag{11}$$

where P_S and Q_S are the stator active and reactive powers, respectively, δ is the load angle, U_S is the stator voltage, I_R is the rotor current, and X_S and X_M are the stator reactance and mutual reactance of the DFIG, respectively.

The power output capability is limited by the maximum allowable currents of the stator and rotor and the steady state stability limit of the DFIG [26]. This can be represented as

$$P_S^2+Q_S^2\leqslant(3U_S I_{S\max})^2 \tag{12}$$

$$P_S^2+(Q_S^2+3\frac{U_S^2}{X_S})^2\leqslant(3\frac{X_M}{X_S}U_S I_{R\max})^2 \tag{13}$$

where $I_{S\max}$ and $I_{R\max}$ are the maximum allowable currents of the stator and rotor, respectively.

Fig. 3 shows the three limits in the PQ plane. According to (12), the stator current limit is indicated by the red dotted semicircle centered at the origin with a radius of $3U_S I_{S\max}$. The rotor current limit (13) is represented by the blue dotted semicircle centered at $(-3U_S^2/X_S, 0)$ with a radius of $3(X_M/X_S)\,U_S I_{R\max}$. According to (10), when the load angle varies from 0° to 90° at constant rotor current and stator voltage, active power increases with the load angle. This results in stable operation points. Thus, the steady state stability limit is denoted by the purple dotted vertical line at $(-3U_S^2/X_S, 0)$. Finally, the power output capability limit can be obtained by adding the rotor active power and stator active power, and it is indicated by the black solid curve in Fig. 3. As $I_{S\max}$, $I_{R\max}$, X_S, and X_M are constants, the reactive power capacity of the DFIG is influenced by active power and terminal voltage.

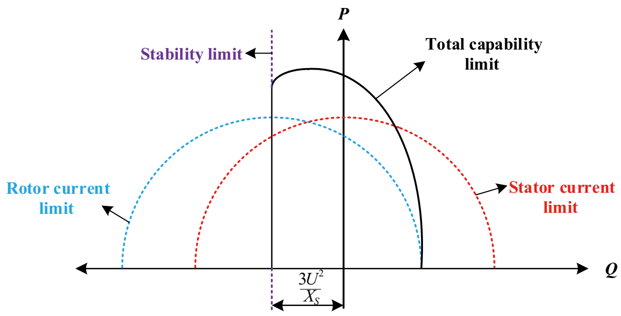

Fig. 3 Power output capability of DFIG

4.2 Predictive model of PVA

(1) State space of PVA

In steady state, the power control behavior of a PVA can be expressed as a first-order function,

$$\Delta P_{PV} = \frac{1}{1+s\tau_{PV}^{P}} \Delta P_{PV}^{ref} \tag{14}$$

$$\Delta Q_{PV} = \frac{1}{1+s\tau_{PV}^{Q}} \Delta Q_{PV}^{ref} \tag{15}$$

τ_{PV}^{P} and τ_{PV}^{Q} are time constants, which are within 100 ms [27].

Then, the state space of the PVA can be derived as

$$\Delta \dot{P}_{PV} = A_{PV}^{P} \Delta P_{PV} + B_{PV}^{P} \Delta P_{PV}^{ref} \tag{16}$$

$$\Delta \dot{Q}_{PV} = A_{PV}^{Q} \Delta Q_{PV} + B_{PV}^{Q} \Delta Q_{PV}^{ref} \tag{17}$$

where $A_{PV}^{P} = -1/\tau_{PV}^{P}$, $B_{PV}^{P} = 1/\tau_{PV}^{P}$, $A_{PV}^{Q} = -1/\tau_{PV}^{Q}$, and $B_{PV}^{Q} = 1/\tau_{PV}^{Q}$.

(2) Reactive power capability of PV inverters

According to the theorem in [28], the power capability of PV inverters is determined by the maximum operating temperature of all semiconductor devices of PV inverters. Based on the operating temperature limitation and the relationship between active power P, reactive power Q, and apparent power S, the constraint model of the inverter power output can be formulated as

$$\frac{P^2}{S^2} + \frac{Q^2}{(k \cdot S)^2} \leqslant 1 \tag{18}$$

where k is the factor for the reactive power constraint. k depends on the topology, the modulation of PV inverters and the semiconductors.

Based on (18), the power output capability of PV inverters is indicated by the half-elliptical curve shown in Fig. 4. The maximum value of active power, P_{max}, is equal to S. Fig.4 shows that the reactive power capability of PV inverters is influenced by parameter k and the active power output. For example, when active power is P_1, the maximum reactive power is Q_1.

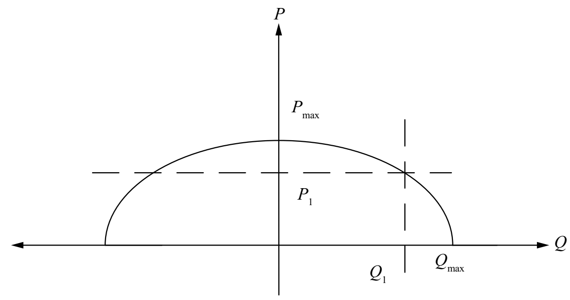

Fig. 4 Power output capability of PV inverters

4.3 Predictive model of STATCOM

The reactive power control behavior of a STATCOM can also be expressed as a first-order function,

$$\Delta Q_{ST} = \frac{1}{1+s\tau_{ST}} \Delta Q_{ST}^{ref} \tag{19}$$

where τ_{ST} is the time constant, and it is within 10 ms.

The state space model of a STATCOM can be derived as

$$\Delta \dot{Q}_{ST} = A_{ST} \Delta Q_{ST} + B_{ST} \Delta Q_{ST}^{ref} \tag{20}$$

where $A_{ST} = -1/\tau_{ST}$ and $B_{ST} = 1/\tau_{ST}$.

4.4 Predictive model of the entire system

The predictive model of the entire system, which consists of N_{WT} WTGs, N_{PV} PVAs, and one STATCOM, can be formulated in the following form:

$$\Delta \dot{\boldsymbol{x}} = \boldsymbol{A} \Delta \boldsymbol{x} + \boldsymbol{B} \Delta \boldsymbol{u} \tag{21}$$

where

$$\begin{aligned} \Delta \boldsymbol{x} = [&\Delta Q_{ST}, \Delta P_{WT_1}, \dots, \Delta P_{WT_{N_{WT}}}, \Delta Q_{WT_1}, \dots, \Delta Q_{WT_{N_{WT}}}, \\ &\Delta P_{PV_1}, \dots, \Delta P_{PV_{N_{PV}}}, \Delta Q_{PV_1}, \dots, \Delta Q_{PV_{N_{PV}}}]^T \end{aligned}$$

$$\begin{aligned} \Delta \boldsymbol{u} = [&\Delta Q_{ST}^{ref}, \Delta P_{WT_1}^{ref}, \dots, \Delta P_{WT_{N_{WT}}}^{ref}, \Delta Q_{WT_1}^{ref}, \dots, \Delta Q_{WT_{N_{WT}}}^{ref}, \\ &\Delta P_{PV_1}^{ref}, \dots, \Delta P_{PV_{N_{PV}}}^{ref}, \Delta Q_{PV_1}^{ref}, \dots, \Delta Q_{PV_{N_{PV}}}^{ref}]^T \end{aligned}$$

$$\boldsymbol{A} = \begin{bmatrix} A_{ST} & & & & \\ & \boldsymbol{A}_{WT}^{P} & & & \\ & & \boldsymbol{A}_{WT}^{Q} & & \\ & & & \boldsymbol{A}_{PV}^{P} & \\ & & & & \boldsymbol{A}_{PV}^{Q} \end{bmatrix}$$

$$\boldsymbol{B} = \begin{bmatrix} B_{ST} & & & & \\ & \boldsymbol{B}_{WT}^{P} & & & \\ & & \boldsymbol{B}_{WT}^{Q} & & \\ & & & \boldsymbol{B}_{PV}^{P} & \\ & & & & \boldsymbol{B}_{PV}^{Q} \end{bmatrix}$$

with

$$\boldsymbol{A}_{WT}^{P} = diag(-1/\tau_{WT_1}^{P}, \dots, -1/\tau_{WT_{N_{WT}}}^{P}),$$

$$\boldsymbol{B}_{WT}^{P} = diag(1/\tau_{WT_1}^{P}, \dots, 1/\tau_{WT_{N_{WT}}}^{P}),$$

$$\boldsymbol{A}_{WT}^{Q} = diag(-1/\tau_{WT_1}^{Q}, \dots, -1/\tau_{WT_{N_{WT}}}^{Q}),$$

$$\boldsymbol{B}_{WT}^{Q} = diag(1/\tau_{WT_1}^{Q}, \dots, 1/\tau_{WT_{N_{WT}}}^{Q}),$$

$$\boldsymbol{A}_{\boldsymbol{PV}}^{\boldsymbol{P}} = diag(-1/\tau_{PV_1}^{P},\ldots,-1/\tau_{PV_{N_{PV}}}^{P}),$$
$$\boldsymbol{B}_{\boldsymbol{PV}}^{\boldsymbol{P}} = diag(1/\tau_{PV_1}^{P},\ldots,1/\tau_{PV_{N_{PV}}}^{P}),$$
$$\boldsymbol{A}_{\boldsymbol{PV}}^{\boldsymbol{Q}} = diag(-1/\tau_{PV_1}^{Q},\ldots,-1/\tau_{PV_{N_{PV}}}^{Q}) \text{ and}$$
$$\boldsymbol{B}_{\boldsymbol{PV}}^{\boldsymbol{Q}} = diag(1/\tau_{PV_1}^{Q},\ldots,1/\tau_{PV_{N_{PV}}}^{Q})$$

Suppose the sampling period is ΔT_S, the continuous model can be transformed into the discrete state space model,

$$\Delta\boldsymbol{x}(k+1) = \boldsymbol{G}\Delta\boldsymbol{x}(k) + \boldsymbol{H}\Delta\boldsymbol{u}(k) \tag{22}$$

where $\boldsymbol{G}$ and $\boldsymbol{H}$ can be obtained by discretizing $\boldsymbol{A}$ and $\boldsymbol{B}$, respectively,

$$\boldsymbol{G} = \mathrm{e}^{\boldsymbol{A}\Delta T_S} \tag{23}$$

$$\boldsymbol{H} = \int_0^{\Delta T_S} \mathrm{e}^{\boldsymbol{A}\tau}\boldsymbol{B}d\tau \tag{24}$$

5 Formulation of MPC problem

In this section, the MPC problem is formulated for the voltage control of the renewable energy power plant. The basic principle, cost functions, and constraints of the MPC problem are described in detail.

5.1 Basic principle of the MPC problem

MPC is also known as receding horizon control (RCH). Fig. 5 shows the principle of MPC.

First, a system prediction model must be established to predict the future dynamics of the system. The red dotted line in the figure represents the predicted state variables obtained according to the system prediction model and current measurements. The predicted state variables are used to formulate the MPC problem. In the process of solving the MPC problem, an optimization problem is solved in the prediction period,ΔT_P, based on the current measurements at each control point. The green dotted line in the figure represents the obtained control sequence. Only the first element of the control sequence is applied to the controller, and control actions are maintained within the control period, ΔT_C [29]. The above process is repeated at the next control point based on new measurements.

Thus, the MPC method considers the future dynamics of the system and uses new measurements for each optimization calculation. This improves voltage control performance. However, the time constants of different reactive power compensation devices can vary considerably. Thus, each control period is divided into several sampling periods to accurately capture the fast dynamics of Var devices with small time constants.

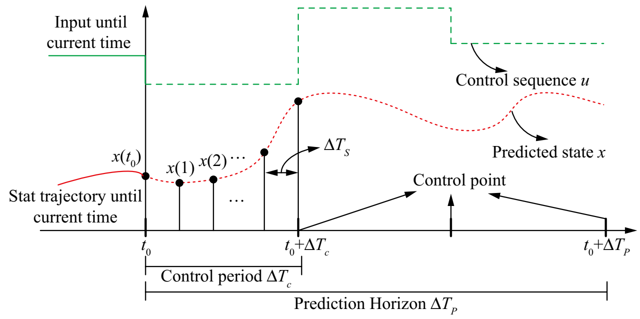

Fig. 5 Principle of the MPC

5.2 Cost function

The control objective of the proposed control strategy is to maintain the voltages of the POC, WTGs, and PVAs within a feasible range and reduce voltage fluctuations.

(1) Objective 1: The active power output fluctuations of wind farms and PV power stations can result in a voltage limit violation at the POC. Thus, the predicted voltage deviation at the POC, ΔV_{POC}^{pre}, with respect to the reference value at the POC, V_{POC}^{ref}, is minimized. This can be expressed as

$$Obj_{V_{POC}} = \sum_{k=1}^{N_P}\left\|\Delta V_{POC}^{pre}(k)\right\|^2 \tag{25}$$

where $N_P = \Delta T_P/\Delta T_S$ is the number of prediction steps.

(2) Objective 2: According to the theorem in [30], the voltages of the five medium voltage (MV) buses shown in Fig. 1 can reflect the voltage conditions of the corresponding subzone. Then, the deviation between the predicted voltages of the MV buses and their reference values are minimized,

$$Obj_{V_{MW}} = \sum_{k=1}^{N_P}\left\|\Delta\boldsymbol{V}_{\boldsymbol{MV}}^{\boldsymbol{pre}}(k)\right\|^2 \tag{26}$$

where $\Delta\boldsymbol{V}_{\boldsymbol{MV}}^{\boldsymbol{pre}} = [\Delta V_{MV_1}^{pre},\Delta V_{MV_2}^{pre},\ldots,\Delta V_{MV_5}^{pre}]^T$.

(3) Objective 3: Finally, the voltages of the WTGs and PVAs are optimized as follows:

$$Obj_{V_{WP}} = \sum_{k=1}^{N_P}\left\|\Delta\boldsymbol{V}_{\boldsymbol{WT}}^{\boldsymbol{pre}}(k)+\Delta\boldsymbol{V}_{\boldsymbol{PV}}^{\boldsymbol{pre}}(k)\right\|^2 \tag{27}$$

The deviation between the predicted voltage and the corresponding reference value can be calculated by

$$\begin{aligned}\Delta V^{pre}(k) &= V(t_0) - V^{ref} + \frac{\partial V}{\partial Q_{ST}}\Delta Q_{ST}(k)\\ &+\frac{\partial V}{\partial P_{WT}}\Delta P_{WT}(k) + \frac{\partial V}{\partial Q_{WT}}\Delta Q_{WT}(k)\\ &+\frac{\partial V}{\partial P_{PV}}\Delta P_{PV}(k) + \frac{\partial V}{\partial Q_{PV}}\Delta Q_{PV}(k)\end{aligned} \tag{28}$$

where $\Delta V^{pre}(k)$can be replaced by ΔV_{POC}^{pre}, ΔV_{MV}^{pre}, ΔV_{WT}^{pre}, and ΔV_{PV}^{pre}. $V(t_0)$is the voltage measured at the current time.

According to (25)–(27), the cost function can be expressed as

$$\min(w_{V_{POC}} \cdot Obj_{V_{POC}} + w_{V_{MV}} \cdot Obj_{V_{MV}} + w_{V_{WP}} \cdot Obj_{V_{WP}}) \tag{29}$$

where $w_{V_{POC}}$, $w_{V_{MV}}$, and $w_{V_{WP}}$ are the weighting factors calculated using the AHP.

5.3 Constraints

(1) Constraints of STATCOM, WTGs, and PVAs

The power outputs of the WTGs, PVAs, and STATCOM are constrained as follows:

$$Q_{ST}^{\min} \leqslant Q_{ST}(k) \leqslant Q_{ST}^{\max} \tag{30}$$

$$\begin{gathered} 0 \leqslant P_{WT_i}(k) \leqslant P_{WT_i}^{avi}, \\ Q_{WT_i}^{\min} \leqslant Q_{WT_i}(k) \leqslant Q_{WT_i}^{\max}, \\ i = 1, 2 \ldots, N_{WT} \end{gathered} \tag{31}$$

$$\begin{gathered} 0 \leqslant P_{PV_n}(k) \leqslant P_{PV_n}^{avi}, \\ Q_{PV_n}^{\min} \leqslant Q_{PV_n}(k) \leqslant Q_{PV_n}^{\max}, \\ n = 1, 2 \ldots, N_{PV} \end{gathered} \tag{32}$$

where $P_{WT_i}^{avi}$ and $P_{PV_n}^{avi}$ are the available active power outputs of the WTGs and PVAs respectively, $Q_{WT_i}^{\min}$ and $Q_{WT_i}^{\max}$ are the minimum and maximum reactive power capacities of the WTGs respectively, and $Q_{PV_n}^{\min}$ and $Q_{PV_n}^{\max}$ are the minimum and maximum reactive power capacities of the PVAs, respectively. Based on the analysis described in Section 4, $Q_{WT_i}^{\min}$, $Q_{WT_i}^{\max}$, $Q_{PV_n}^{\min}$, and $Q_{PV_n}^{\max}$ can be obtained considering actual operating conditions.

(2) System constraints

The active power output references of the wind farm and PV station, P_{WF}^{ref} and P_{PVS}^{ref}, specified by a system operator must be tracked. These power output references can be expressed as follows:

$$\sum_{i=1}^{N_{WT}} P_{WT_i}^{ref} = P_{WF}^{ref} \tag{33}$$

$$\sum_{i=1}^{N_{PV}} P_{PV_i}^{ref} = P_{PVS}^{ref} \tag{34}$$

The formulated MPC problem can be transformed to a standard QP problem, which can be solved by commercial QP solvers in milliseconds [31].

6 Case studies

A power plant with 80 WTGs, 20 PVAs, and a ±180 MVar STATCOM connected to a WSPG is used to verify the proposed coordinated voltage control strategy. To reflect the characteristics of the WSPG, the short-circuit capacity provided by the external power grid at the POC is set as 540 MVA. The simulation model is built in the MATLAB/Simulink environment.

The objective of the coordinated voltage control strategy is to control the voltages of the POC, WTGs, and PVAs within a reasonable range when the active power output of the renewable energy power plant fluctuates. Voltage control performance is examined using the simulation model. The total simulation time is 180 s.

Fig. 6 shows the active power references of the wind farm and PV station. The wind farm operation mode is changed from the balance control mode to maximum power point tracking (MPPT) mode during the simulation. The PV station operates in the MPPT mode.

Fig. 7 and 8 show the voltage of the POC and WTG_80 for two control strategies (coordinated voltage control (CVC) and no control (NC)). Under NC, only the STATCOM

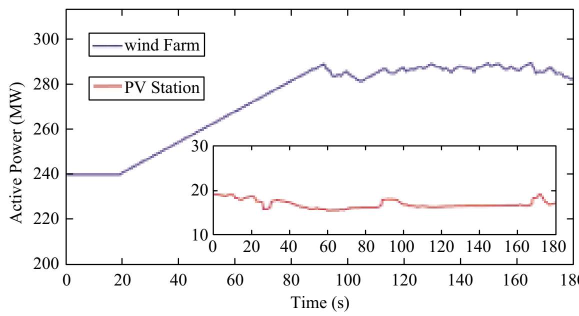

Fig. 6 Active power references of wind farm and PV station

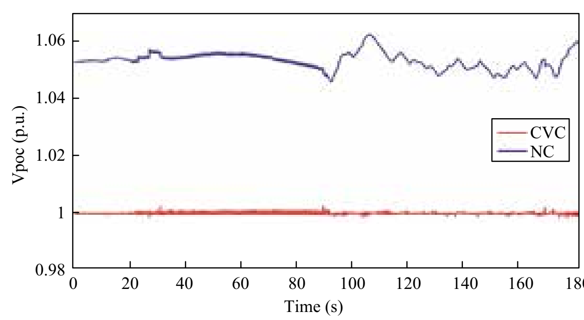

Fig. 7 Voltage of POC

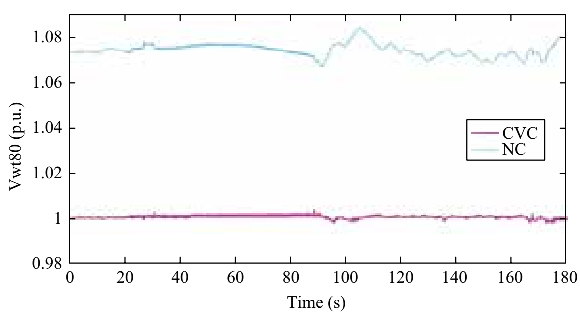

Fig. 8 Voltage of WTG_80

is controlled and the WTGs and PVAs work under a unit power factor. The proposed voltage control strategy effectively reduces voltage fluctuation and maintains voltage at almost 1 p.u. The voltage of the POC and of each generation unit inside the renewable energy power station are optimized.

Fig. 9 shows the reactive power outputs of the STATCOM, WTG_80, and PVA_20. As the active power output increases, the reactive power output of the STATCOM increases to maintain the balance of reactive power. The reactive power outputs of the WTGs and PVAs are also optimized to improve voltage control performance.

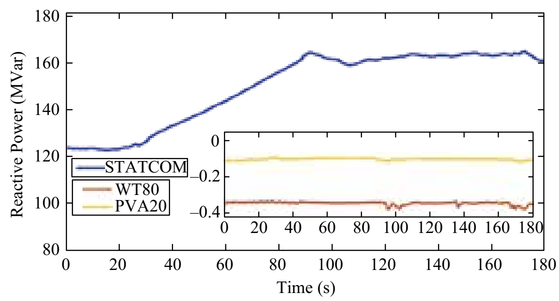

Fig. 9 Reactive power outputs of STATCOM, WTG_80, and PVA_20

Voltage control performance is observed under different short-circuit ratios (SCRs), i.e., 1.5, 2.5, and 5.0.

Fig. 10 shows the voltage control performance of the proposed strategy at different SCRs. The proposed strategy can maintain the voltage of the POC within a reasonable range at all SCRs. As the SCR increases, the voltage fluctuation at the POC decreases. The reactive power output of the STATCOM at different SCRs is shown in Fig. 11. As the SCR increases, the reactive power output of the STATCOM decreases. This increases reactive power reserves. This is because as the SCR increases, the short-circuit capacity of the external power grid and the reactive power support capacity increase.

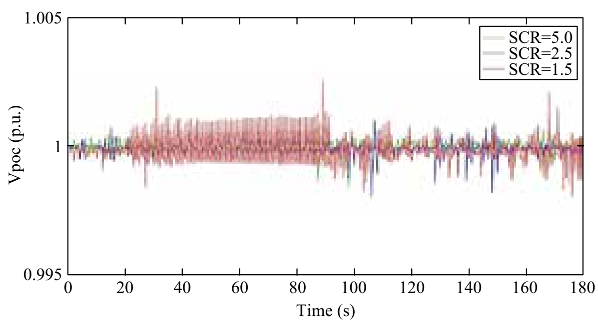

Fig. 10 Voltage of POC at different SCRs

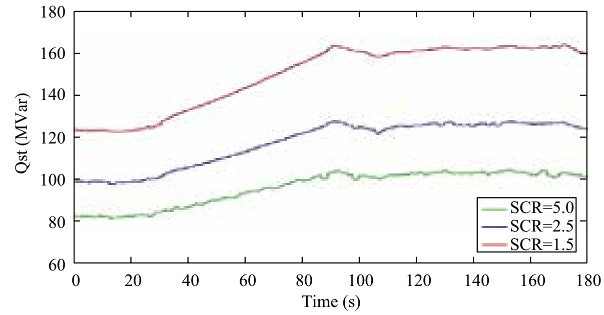

Fig. 11 Reactive power output of STATCOM at different SCRs

Two scenarios are considered to analyze the influence of the time delay on voltage control performance. In scenario 1 (S1), the time constants of the active and reactive power control loops of the WTG (τ_{WT}^{P} and τ_{WT}^{Q}) are set as 1 s and 5 s, respectively. In scenario 2 (S2), τ_{WT}^{P} and τ_{WT}^{Q} are set as 2 s and 8 s, respectively. Fig. 12 shows the voltage of the POC in both scenarios. Voltage fluctuation is smaller in S1. When the time delay is large, the local controllers of the WTGs require more time to track the power output reference values given by the MPC controller. In the control period, the actual power outputs may differ significantly from reference values. This leads to poor voltage control performance. Therefore, voltage control performance is better when the time delay is small.

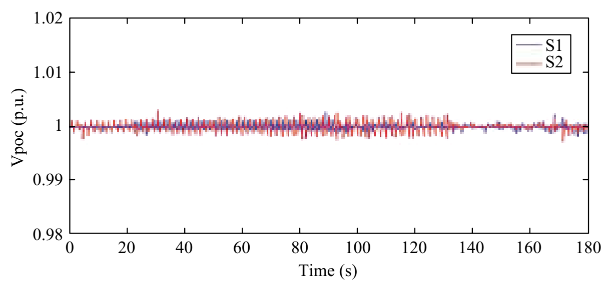

Fig. 12 Voltage of POC at different time delays

7 Conclusions

MPC-based coordinated voltage control is developed to optimize the voltage of a renewable energy power plant connected to a WSPG. Active power is controlled in addition to reactive power. The reactive power capability of WTGs and PVAs is examined. In the proposed voltage control strategy, power regulation devices with different time constants, i.e., a STATCOM, WTGs, and PVAs, are coordinated to maintain voltage within a reasonable range. Case studies show the coordinated voltage control strategy exhibits good voltage control performance, which improves the voltage quality of the entire power plant. The proposed control strategy only contains voltage control objectives. More control objectives will be considered in future work.

Acknowledgements

This work was supported by National Natural Science Foundation Joint Key Project of China (2016YFB0900900).

References

[1] Ma J, Zhao D, Qian M, Zhu L, Yao L, Wang N (2017) Reviews of control technologies of large-scale renewable energy connected to weakly-synchronized sending-end DC power grid. Power System Technology, 41(10): 3112-3120

[2] Neumann T, Feltes C, Erlich I (2011) Response of DFG-based wind farms operating on weak grids to voltage sags. In: IEEE Power and Energy Society General Meeting, Detroit, MI, USA, 1-6 July 2011

[3] Xue Y, Lei X, Xue F, Yu C, et al (2014) A review on impacts of wind power uncertainties on power systems. Proceedings of the Chinese Society of Electrical Engineering, 34(29): 5029-5040

[4] Ding M, Wang W, Wang X, et al (2014) A review on the effect of large-scale PV generation on power systems. Proceedings of the Chinese Society of Electrical Engineering, 34(1): 1-14

[5] Wu Q, Xu Z, Jacob Østergaard (2010) Grid integration issues for large scale wind power plants (WPPs). In: IEEE PES General Meeting, Providence, RI, USA, 25-29 July 2010

[6] Guo Q, Sun H, Wang B, et al (2015) Hierarchical automatic voltage control for integration of large-scale wind power: Design and implementation. Electric Power Systems Research, 120: 234-241

[7] Chen Z, Guerrero JM, Blaabjerg F (2009) A review of the state of the art of power electronics for wind turbines. IEEE Transactions on Power Electronics, 24(8): 1859-1875

[8] Hansen AD, Sørensen PE, Iov F, Blaabjerg F (2006) Centralized power control of wind farm with doubly fed induction generators. Renewable Energy, 31(7): 935-951

[9] Karthikeya B, Schutt R (2014) Overview of wind park control strategies. IEEE Transactions on Sustainable Energy, 5(2): 416-422

[10] Zhang C, Xu Y, Dong Z, Ravishankar J (2019) Three-stage robust inverter-based voltage/var control for distribution networks with high-level PV. IEEE Transactions on Smart Grid, 10(1): 782-793

[11] Cao N, Jin D, Song Z, Chong K, Qi L (2017) Study on adaptive voltage control strategy of double-fed wind farm. In: Chinese Automation Congress, Jinan, China, 3565-3570 October 2017

[12] Li R, Tang F, Liu Y, et al (2012) A new scheme of reactive power compensation and voltage control for DFIG based wind farm. Proceedings of the Chinese Society of Electrical Engineering, 32(19): 16-23

[13] Qiao W, Harley RG, Venayagamoorthy GK (2009) Coordinated reactive power control of a large wind farm and a STATCOM using heuristic dynamic programming. IEEE Transactions on Energy Conversion, 24(2): 493-503

[14] Tang Y, He H, Ni Z, Wen J, Sui X (2014) Reactive power control of grid-connected wind farm based on adaptive dynamic programming. Neurocomputing, 125: 125-133

[15] DÍaz-Dorado E, Carrillo C, CidrÁs J (2008) Control algorithm for coordinated reactive power compensation in a wind park. IEEE Transactions on Energy Conversion, 23(4): 1064-1072

[16] Schonleber K, Collados C, Pinto RT, Rates-Palau R, Gomis-Bellmunt O (2017) Optimization-based reactive power control in HVDC-connected wind power plants. Renewable Energy, 109: 500-509

[17] Zhang B, Hou P, Hu W, et al (2016) A reactive power dispatch strategy with loss minimization for a DFIG-based wind farm. IEEE Transactions on Sustainable Energy, 7(3): 914-923

[18] Sakamuri JN, Rather ZH, Rimez J, et al (2016) Coordinated voltage control in offshore HVDC connected cluster of wind power plants. IEEE Transactions on Sustainable Energy, 7(4): 1592-1601

[19] Schönleber K, Ratés-Palau S, Gomis-Bellmunt O (2017) Analysis of reactive power strategies in HVDC-connected wind power plant clusters. Wind Energy, 20(12): 1971-1982

[20] Xu F, Guo Q, Sun H, et al (2015) Automatic voltage control of wind farms based on model predictive control theory. Automation of Electric Power Systems, 39(7): 59-67

[21] Zhang Z, Wang C, Dong X, et al (2019) Coordinated voltage control strategy of wind farms based on hierarchical model predictive control. Automation of Electric Power Systems, 43(11): 34-42

[22] Zhao H, Wu Q, Guo Q, et al (2016) Coordinated voltage control of a wind farm based on model predictive control. IEEE Transactions on Sustainable Energy, 7(4): 1440-1451

[23] Christakou K, LeBoudec J, Paolone M, Tomozei DC (2013) Efficient computation of sensitivity coefficients of node voltages and line currents in unbalanced radial electrical distribution networks. IEEE Transactions on Smart Grid, 4(2): 741-750

[24] Guo Y, Gao H, Wu Q, et al (2018) Enhanced voltage control of VSC-HVDC-connected offshore wind farms based on model predictive control. IEEE Transactions on Sustainable Energy, 9(1): 474-487

[25] Larsen EV, Achilles AS (2013) System and method for voltage control of wind generators. US Patent App. 14/018,482, Sept 2013

[26] Santos-Martin D, Arnaltes S, Amenedo JLR (2018) Reactive power capability of doubly fed asynchronous generators. Electric Power Systems Research, 78(11): 1837-1840

[27] Yan W, Wang S, Liu X, Shen D (2019) System level PV fast power control technology and application. Proceedings of the Chinese Society of Electrical Engineering, 39: 213-224

[28] Ma L, Xu Y, Huang AQ (2018) A study of physical limitation of reactive power output capability of modern PV inverters. In: IEEE/PES Transmission and Distribution Conference and Exposition (T&D), Denver, CO, USA, 16-19 April 2018

[29] Camponogara E, Jia D, Krogh BH, Talukdar S (2002) Distributed model predictive control. IEEE Control Systems Magazine, 22(1): 44-52

[30] Lagonotte P, Sabonnadiere JC, Leost JY, Paul JP (1989)

Structural analysis of the electrical system: Application to secondary voltage control in France. IEEE Transactions on Power Systems, 4(2): 479-486

[31] Wang Y, Boyd S (2010) Fast model predictive control using online optimization. IEEE Transactions on Control Systems Technology, 18(2): 267-278

Biographies

Yongning Chi received a Ph.D. degree from China Electric Power Research Institute (CEPRI), Beijing, in 2006. He has been employed at CEPRI since 2006, presently as Chief Engineer of Renewable Energy Department of CEPRI. His most recent research involves integration of large scale wind power into the Chinese power grid and grid code development. His primary fields of interest are wind power integration impact on power system and power system stability analysis.

Weihao Li received a B.S degree from North China Electric Power University, Baoding, in 2017. He is working towards M.S degree at Shandong University, Jinan. His research interests include power system analysis and renewable energy.

Qiuwei Wu obtained the B. Eng. and M. Eng. in Power System and Its Automation from Nanjing University of Science and Technology, Nanjing, China, in 2000 and 2003, respectively. He obtained the PhD degree in Power System Engineering from Nanyang Technological University, Singapore, in 2009. He was a senior R&D engineer with Vestas Technology R&D Singapore Pte Ltd from Mar. 2008 to Oct. 2009. He has been working at Department of Electrical Engineering, Technical University of Denmark (DTU) since Nov. 2009 (PostDoc Nov. 2009-Oct. 2010, Assistant Professor Nov. 2010-Aug. 2013, Associate Professor since Sept. 2013). He was a visiting scholar at Department of Industrial Engineering & Operations Research (IEOR), University of California, Berkeley, from Feb. 2012 to May 2012 funded by the Danish Agency for Science, Technology and Innovation (DASTI), Denmark. He has been a visiting professor named by Y. Xue, an Academician of Chinese Academy of Engineering, at Shandong University, China, since Nov. 2015. His research interests are modeling and control of wind power, electric vehicle, active distribution networks, energy management, and electricity market.

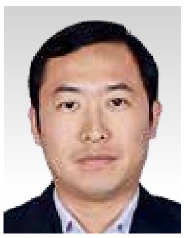

Chao Liu received a M.S. degree at Shandong University, Jinan, 2009, and received B.S. degree at Shandong University, Jinan, 2006. He is working in China Electric Power Research Institute, Beijing. His research interests include renewable energy generation and integration.

(Editor Dawei Wang)